Hygrothermal Aging of Rubber-Modified and Mineral-Filled Dicyandiamide-Cured DGEBA Epoxy Resin. III. Dielectric Spectroscopy Investigation

KATYA I. IVANOVA, RICHARD A. PETHRICK, S. AFFROSSMAN

Department of Pure and Applied Chemistry, University of Strathclyde, Thomas Graham Building, 295 Cathedral Street, Glasgow G1 1XL, UK

Received 12 June 2001; accepted 18 July 2001

ABSTRACT: The effects of moisture absorption on the dielectric properties of a rubber-modified, mineral-filled, epoxy resin based on the diglycidyl ether of bisphenol A cured with dicyandiamide are reported. Samples of the resin were aged by immersing in deionized water, or 5% w/w NaCl solution, at elevated temperatures. Dielectric measurements were carried out over the frequency range 10^{-1} to 6×10^5 Hz. A featureless dielectric spectrum was observed with both real and imaginary dielectric permittivity increasing with the amount of absorbed water. The change in the dielectric properties with absorption of water was independent of presence of salt, temperature of exposure, and aging history, although a hysteresis of the hydration–dehydration process was observed at low frequencies. Two types of absorbed water were observed—water molecularly dispersed within the epoxy matrix and clustered water in spherical microcavities. The time dependence of the real dielectric permittivity measured at 10 kHz was found to closely resemble that of the water absorption, which allowed the activation energy of diffusion to be calculated from both dielectric and gravimetric data. © 2002 Wiley Periodicals, Inc. J Appl Polym Sci 84: 1011–1024, 2002; DOI 10.1002/app.10368

Key words: dielectric properties; aging; epoxy resin; water absorption; microcavity formation

INTRODUCTION

Numerous experimental methods are used to study water absorption in materials, for example, gravimetric determination of the weight gain, nuclear magnetic resonance, differential scanning calorimetry, dynamic mechanical thermal analysis, and infrared Fourier transform spectroscopy. Electromagnetic propagation techniques have also been used to characterize the water sorption by a variety of materials.[1] Inductance, resistance, or capacity values can be measured and related to the water content. Measurement of the effective permittivity via time–domain refractometry (TDR) is a popular method for estimating the volumetric water content of soil,[2] and dielectric spectroscopy (DS) has been recently extensively investigated as a method of characterizing the process of cure and sorption of water in epoxy resin matrices.[3]

An immersed polymer can be seen as a two-phase system: filler (water) in a matrix (pure or reinforced polymer). A review on the modeling of such systems can be found in the literature.[4] The dielectric properties of a material are obviously dependent on the water content, but the correlation between the dielectric permittivity and the amount of absorbed water is not simple because many phenomena are involved. Both the state and the amount of water absorbed influence the

Correspondence to: R.A. Pethrick.

Journal of Applied Polymer Science, Vol. 84, 1011–1024 (2002)

dielectric permittivity. Moreover, polarization phenomena of other components in the polymer system can also influence the dielectric properties.

Water in polymers can be molecularly dispersed or clustered. Clustering usually occurs when capillaries and microcavities exist in the polymer. Maxwell and Pethrick[5] compared the dielectric properties of dry and water aged epoxy resins and found two distinct processes. A peak at about 273 K was associated with the freezing of water in cavities, and a lower temperature process was ascribed to water molecules dispersed within the resin and bound to it by hydrogen bonds. However, Woo and Piggott[6] studying DGEBA based epoxy resins concluded that the water does not appear to be bound to polar groups in the resin or hydrogen bonding sites, although dielectric tests indicated that it does not behave as free water because its polarizability is much reduced. The amount of reduction in the effective dielectric constant of the water is about 55 to 77%, indicating that there is some clustering of the water molecules in the polymer, rather than complete separation of the molecules. Aldrich et al.[7] also found that water is not strongly bound to the epoxy matrix. The dielectric permittivity measured at 10 kHz was close to the Onsager predicted value with the water molecules showing roughly 70–100% of their free-state polarizability. The high dielectric constant of liquid water is a consequence of the interactions between the water molecules. For molecularly dispersed water a lower dielectric permittivity applies because interactions between the water molecules do not occur. The dielectric permittivity of bound water is unknown, but it is presumed to lie between the values for ice and liquid water. Bosma et al.[8] studied water absorption by aromatic diamine-cured tetrafunctional epoxy resin with dielectric spectroscopy. A liner relationship between the dielectric permittivity at 10 kHz and the water weight fraction was again observed. They proposed a model based on the assumption of a time-dependent dielectric permittivity of the matrix during the aging, due to swelling, chemical, or other physical modification. Lu et al.,[9] studying polyurethane/alumina powders and polyurethane/carbon fibers composites with dielectric spectroscopy, reported that water is absorbed not only by the polymer matrix but also by the interfaces introduced by the fillers. Etienne et al.[10] observed strong dielectric relaxation effects in polymer-based insulating materials when exposed to moisture due to conductivity effects occurring at the matrix–filler particle interface. These effects were reversible upon drying. Korzhenko et al.[11] studied alpha and Maxwell-Wagner relaxation in polyurethane coatings during exposure to water, and observed an initial decrease in the relaxation time due to plasticization, followed by a decrease of the relaxation time and ionic conductivity associated with formation and growing of blisters. Pethrick et al.[12,13] obtained the diffusion coefficient for water absorption in epoxy/amine thermosets from dependence of the real dielectric permittivity on the time of exposure to moisture. The results were close to those calculated from the gravimetric data.

This study is concerned with the effect of hydration–dehydration cycling on the dielectric properties of a complex epoxy resin system. The effects of elevated exposure temperatures and the presence of salt are also examined. In previous articles[14,15] the diffusion behavior of water and its effect on the dynamic mechanical properties of the resin were discussed. Anomalous two-stage absorption was observed when the resin was exposed to deionized water. It was found that water absorbed during the first stage of the absorption plasticizes the epoxy matrix and the water absorbed during the second stage resides in microcavities, and does not further suppress the glass transition temperature of the material. Microcavity formation and a second stage of absorption were not observed when the resin was immersed in 5% w/w NaCl solution, which led to the suggestion that the microcavities grow via an osmotic mechanism.

The aim of this article is to describe the changes in the dielectric properties of an epoxy resin that occur with water uptake in conjunction with gravimetric measurements to diagnose the water absorption behavior of the material.

EXPERIMENTAL

Material

The material used was the same as that in previous articles:[14,15] a DGEBA-based epoxy resin, toughened with carboxyl terminated butadiene acrylonitrile rubber, filled with fumed silica and calcium silicate and cured with dicyandiamide. The curing conditions were described in Part I.[14] The material was molded in the form of a disk, 105 mm diameter and 2.6 ± 0.2 mm thick. The

Table I Aging History of Tested Samples

Sample	Aging Conditions	I Sorption Cycle		II Sorption Cycle	
		Hydration Time (h)	Dehydration Time (h)	Hydration Time (h)	Dehydration Time (h)
A	deionized water at 65°C	74	280	4000	400
B	deionized water at 65°C	163	420	5100	445
C	deionized water at 65°C	7250	430	—	—
D	5% w/w NaCl solution at 65°C	74	280	7050	330
E	5% w/w NaCl solution at 65°C	152	280	6850	330
F	5% w/w NaCl solution at 65°C	7700	330	—	—
G	deionized water at 60°C	1000	—	—	—
H	deionized water at 50°C	12,000	—	—	—

disks were dried in an oven at 50°C for a month. A sample with dimensions 40 × 40 mm was cut from each disk; the remaining material was cut into 30 × 10-mm samples that were used for dynamic mechanical thermal analysis. The results from the DMTA were presented in Part II.[15]

Aging Procedure

Six samples were aged by being exposed to deionized water or 5% w/w NaCl solution in sealed jars maintained at a constant temperature of 65°C ± 1°C in an electronically controlled oven. The aging solution was changed on a weakly basis to avoid contamination. At selected times the samples were removed from the deionized water/salt solution and placed in an oven with silica gel at 65°C to allow desorption of water to occur. After reaching equilibrium weight some of the samples were rehydrated and then dried again. The samples were designated A, B, C, D, E, and F. The first three were aged in deionized water and the later in 5% w/w NaCl solution. The same samples were used for the gravimetric study of the water absorption described in Part I.[14] In addition, two samples, designated G and H, were aged in deionized water at 60 and 50°C, respectively. Table I presents the aging regime undergone by the samples during the study.

On a regular basis dielectric spectroscopy measurements were carried out on the samples. Prior to measurement, the conditioned samples were wiped with absorbent paper to remove excess of water and weighed to determine their moisture content.

Dielectric Spectroscopy Measurements—DS

Dielectric measurements were carried out using a Solatron 1250A Frequency Response Analyzer (FRA) operating over the frequency range 10^{-3} to 6×10^5 Hz. The network analyzer output was interfaced to the sample via an inverting amplifier and a charge amplifier on the input. A standard three-terminal cell (Wayne Kerr, Type D321) was used for the measurements. The complex impedance and conductivity of the external circuit were used to calculate the dielectric permittivity ϵ' and dielectric loss ϵ''. The method used and the analysis procedures applied to the data have been discussed previously.[16]

Gravimetric Measurements

The weight of the samples was determined using a Mettler AJ100 electronic balance with accuracy of ±0.1 mg. The time required for the weighing of the samples was considered sufficiently short for water evaporation not to be significant. The water weight fraction, w, was defined as the total weight of water absorbed at a certain moment in time per unit weight "wet" polymer:

$$w = \frac{W_t - W_{\text{initial}}}{W_t} \tag{1}$$

where, W_t is the weight of the sample at a certain moment of time and W_{initial} is the initial weight of the sample. The water volume fraction, v, was defined as the volume of water absorbed at certain moment of time per unit volume "wet" polymer:

$$v = \frac{(W_t - W_{\text{initial}})/\rho_{\text{water}}}{W_{\text{initial}}/\rho_{\text{polymer}}} \tag{2}$$

where ρ_{water} and ρ_{polymer} are the densities of the water and the polymer, respectively. In expression (2) the swelling of the material is neglected.

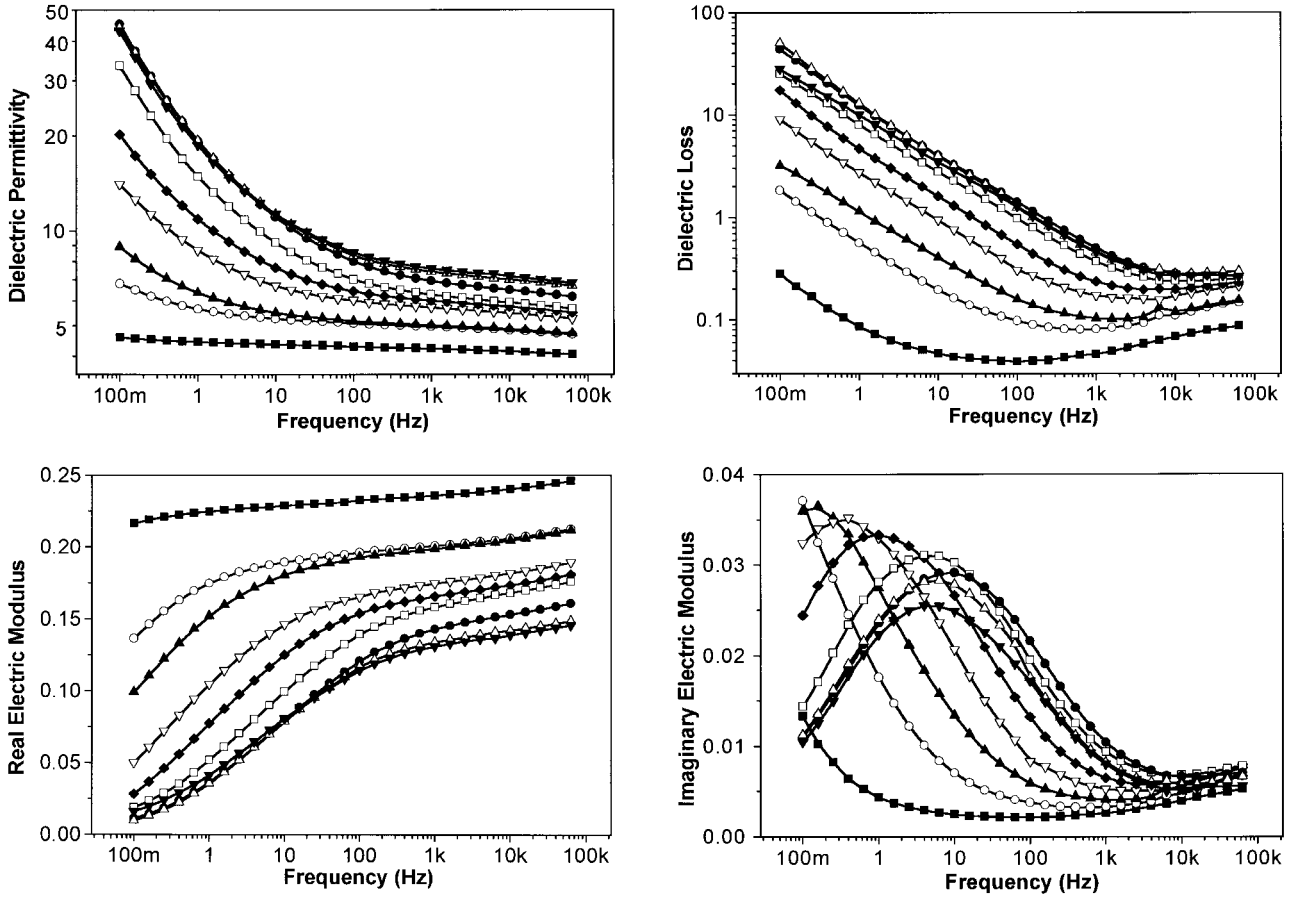

Figure 1 (a) Real and (b) imaginary dielectric permittivity and (c) real and (d) imaginary electric modulii vs. frequency at different stages of ageing of sample C in deionized water at 65°C. (■) represents the data measured before the start of the experiment; (○), (▲), (▽), (◆), (□), (●), (△), and (▼) after 22.25, 74.75, 163, 218, 402, 2146, 6748, and 7250 h of aging, respectively.

RESULTS AND DISCUSSION

The results for the real, ϵ', and imaginary, ϵ'', parts of the dielectric permittivity as a function of frequency at different times of exposure to deionized water are shown in Figure 1(a) and (b), respectively. Both the real and imaginary parts rise sharply toward low frequencies, and the rise is displaced to higher frequencies for longer times of exposure. Both real and imaginary permittivities increase with time of exposure. When the permittivity and loss spectra of a material are featureless, as in this case, it is difficult to separate the interfacial polarization and conductivity contributions to the spectra from the intrinsic dipolar relaxation contributions. This difficulty can be overcome by representing the data in terms of the electric modulus. The complex electric modulus is defined as

$$M^* = 1/\varepsilon^* \tag{3}$$

where ϵ^* is the complex dielectric permittivity. The use of the electric modulus formalism leads to a description of dielectric data, even for materials containing molecular or other types of electrical dipoles, in terms of a distribution of conductivity relaxation times arising from a stretched exponential decay of the electric field under the constraint of a constant displacement vector.[17,18] Analysis of the dielectric data in the M^* representation form is intended to suppress the otherwise overwhelming contribution from interfacial polarization, so that featureless ϵ' and ϵ'' spectra may be resolved into plateaus and peaks in the M' and M'' spectra, which are then related to the limiting high frequency permittivity, ϵ_∞, and the dc conductivity.[19] The disadvantage of the formalism is

that the entire dielectric behavior is described in terms of conductivity relaxation.

The mathematical transformation of ϵ^* to M^* yields,

$$M'_{\text{meas}} \equiv \frac{\varepsilon'_{\text{meas}}}{\varepsilon'^2_{\text{meas}} + \varepsilon''^2_{\text{meas}}} \qquad M''_{\text{meas}} \equiv \frac{\varepsilon''_{\text{meas}}}{\varepsilon'^2_{\text{meas}} + \varepsilon''^2_{\text{meas}}} \tag{4,5}$$

$$M'_{\text{meas}} = \frac{1}{S}(\varepsilon'_{\text{dip}} + \varepsilon'_{\text{int}}) \tag{6}$$

$$M''_{\text{meas}} = \frac{1}{S}(\varepsilon''_{\text{dip}} + \varepsilon''_{\text{dc}} - \varepsilon''_{\text{int}}) \tag{7}$$

where

$$S = \left[\left(\varepsilon'_{\text{dip}} + \varepsilon'_{\text{int}}\right)^2 + \left(\varepsilon''_{\text{dip}} + \frac{\sigma_0}{\omega\varepsilon_0} - \varepsilon''_{\text{int}}\right)^2\right] \tag{8}$$

where the subscripts "int," "dc," and "dip" refer the contributions to the real and imaginary electric permittivity from interfacial polarization, DC conductivity, and dipolar relaxation. The contributions to M' and M'' from interfacial polarization are taken to be negligible on the low-frequency side of the spectra and are therefore ignored, although these contributions distort the shape of the M^* spectrum.

The variation of real and imaginary parts of the electric modulus with frequency at different times of exposure to deionized water are shown in Figure 1(c) and (d), respectively. Both the dispersion in the real part and the incidence of a relaxation peak in the imaginary part are clearly evident. There is a decrease in the magnitude of the plateau region in the real electric modulus and a shift of the peak in the imaginary electric modulus toward higher frequencies with time of exposure.

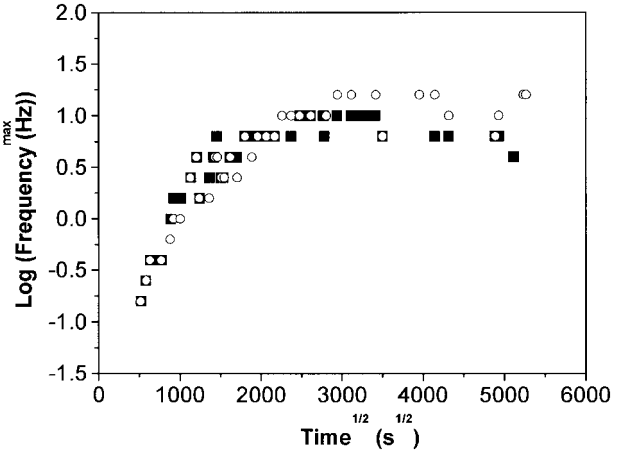

Figure 2 Change in the peak frequency with square root of time of exposure to (■) deionized water and (○) 5% w/w NaCl solution at 65°C.

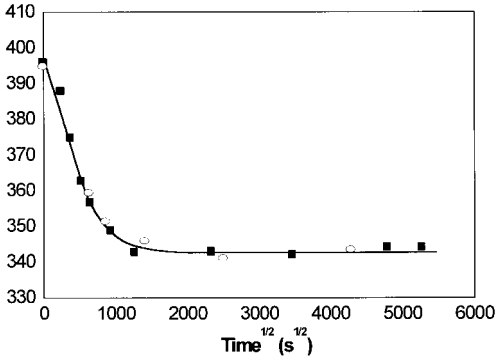

Figure 3 Change in the glass transition temperature with square root of time of exposure to (■) deionized water and (○) 5% w/w NaCl solution at 65°C.

The evolution of the peak frequency with the square root of time of exposure is shown in Figure 2 (solid squares). The sharp increase in the peak frequency during the first 600 h of exposure to deionized water is followed by a plateau region. The peak frequency behavior mirrors the time dependence of the glass transition temperature of the material, illustrated by Figure 3. This correlation reflects the enhanced charge carrier mobility due to the plasticization of the polymer matrix by the absorbed water.

Figure 4 shows the real dielectric permittivity measured at different frequencies as a function of the water weight fraction. The water weight fraction was varied by immersing the material in deionized water at 65°C. The permittivity measured at 10 and 1 kHz depends linearly on the water weight fraction with a correlation factors of 0.99 and 0.98, respectively, while the permittivity measured at frequencies below 1 kHz deviate from linear behavior. It was found that the composition dependence of the real dielectric permittivity is independent of previous history of exposure to deionized water.

For all the samples the dielectric permittivity was monitored as a function of the water weight fraction on both hydration and dehydration, and there was no apparent hysteresis for frequencies above 1 kHz. However, the dielectric permittivity

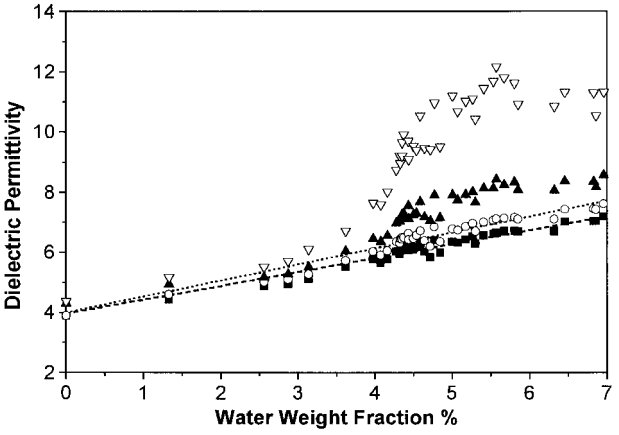

Figure 4 Dielectric permittivity measured at (■) 10 kHz, (○) 1 kHz, (▲) 100 Hz, and (▽) 10 Hz as a function of the water weight fraction. The data were obtained on exposure of sample C to deionized water at 65°C.

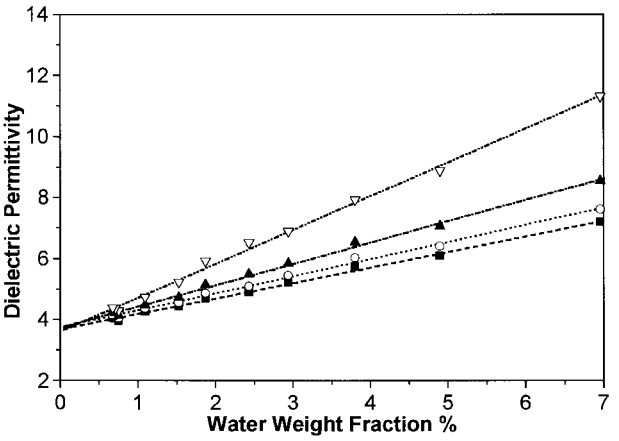

Figure 5 Dielectric permittivity measured at (■) 10 kHz, (○) 1 kHz, (▲)100 Hz, and (▽) 10 Hz as function of the water weight fraction. The data were obtained on dehydration of sample C at 65°C.

measured at frequencies below 1 kHz showed hysteresis relative to the hydration-dehydration cycle.

Figure 5 shows the real dielectric permittivity measured at different frequencies as a function of the water weight fraction, which was varied by drying the material in an oven at 65°C. The real and imaginary electric modulii of the material are given as a function of frequency at different times of dehydration in Figure 6.

It is seen from Figure 5 that the real dielectric permittivity depends linearly with correlation factors of 1, on the water weight fraction at all given frequencies. The slopes of the plots of the dielectric permittivity measured at 1 kHz and 10 kHz vs. water weight fraction are the same as those calculated from the data obtained on hydration. The slope of the dielectric permittivity vs. water fraction plot for 100 and 10 Hz was found to vary with the amount of water absorbed prior to the dehydration process.

A nonuniform distribution of water across the thickness of the sample would give a hysteresis of the dielectric permittivity vs. the water content. The effect of the concentration gradient on the dielectric permittivity calculated from the measured complex capacitance can be evaluated by considering a serial model built up of layers with different amounts of homogeneously dispersed water (Fig. 7). For a serial model the apparent dielectric permittivity is

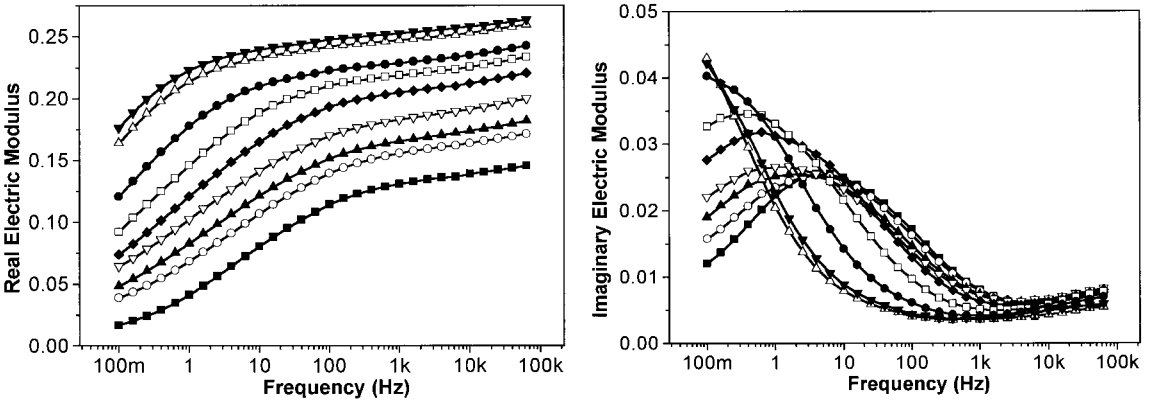

Figure 6 (a) Real and (b) imaginary electric modulii vs. frequency at different stages of dehydrating of sample C at 65°C. (■) represents the data measured after 7250 h aging in deionized water at 65°C; (○), (▲), (▽), (◆), (□), (●), (△) and (▼) after 23, 49.5, 77, 120, 143, 192, 311, and 430 h of dehydration, respectively.

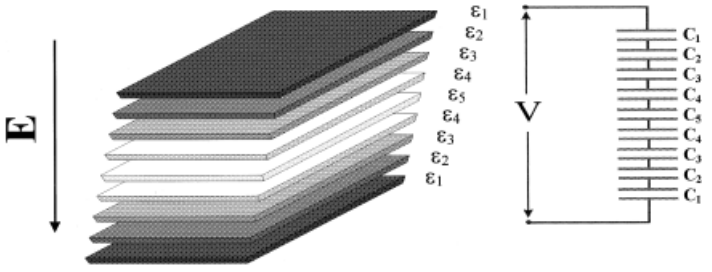

Figure 7 Representation of the serial model.

$$\frac{1}{\langle \varepsilon \rangle} = \frac{1}{n} \cdot \sum_{i=1}^{n} \frac{1}{\varepsilon_i} \tag{9}$$

where ϵ_i is the dielectric permittivity of the ith layer.

Figure 8 shows the computer generated 3D plot of the normalized water concentration as a function of time and distance from the surface of a semi-infinite sample for Fickian diffusion with a constant diffusion coefficient. Figure 8(a) and (b) show the absorption and desorption parts of the plot, respectively. These results were then used to model the change of the apparent dielectric permittivity with time of sorption, related to the total amount of water in the system.

A linear connection between the dielectric increment and the water content was assumed

$$\varepsilon_i^{(\mathrm{wet})}(t) - \varepsilon^{(\mathrm{dry})} = k c_i(t) \tag{10}$$

where $\epsilon_i^{(\mathrm{wet})}(t)$ is the dielectric permittivity of the "wet" layer i at a fixed distance from the surface at certain moment of time t, $\epsilon^{(\mathrm{dry})}$ is the dielectric permittivity of the dry material, $c_i(t)$ is the water content of the ith layer at time t, and k is a coefficient of proportionality.

The computer-simulated results for the composition dependence of the apparent dielectric permittivity, calculated for different k are given in Figure 9. It is evident that for small dielectric increments, i.e. higher frequencies, there is no significant hysteresis relative to the hydration–dehydration cycle, and there is a strong hysteresis for great increments, i.e., low frequencies.

Figure 10 shows the real and imaginary parts of the electric modulus as a function of frequency for different times of immersing in 5% w/w NaCl solution at 65°C. The traces are very similar to those when the material is immersed in deionized water.

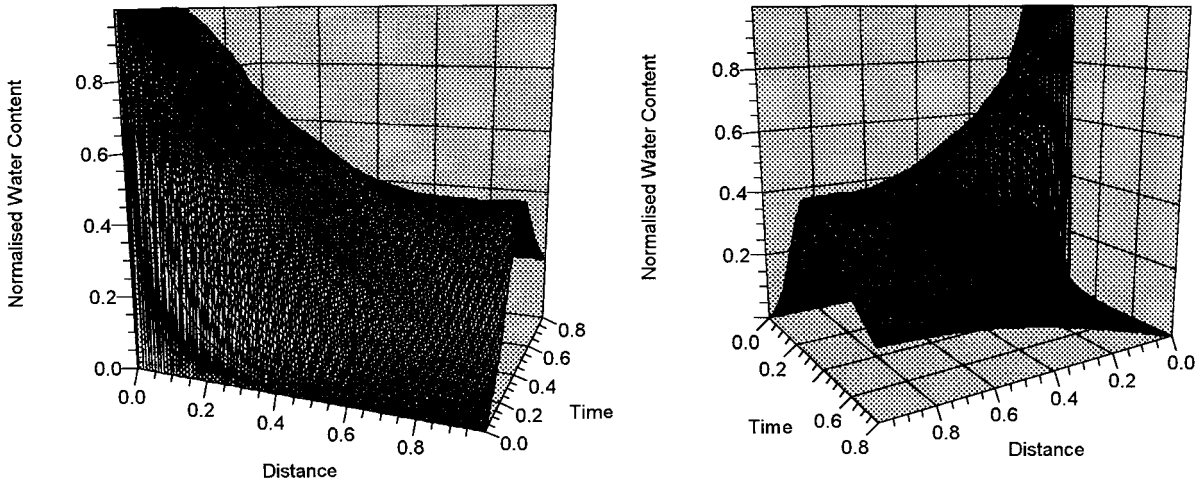

Figure 8 3D plot of the water content at different times and different distances from the surface of semi-infinite sample, obtained with Fickian model of absorption for a constant diffusion coefficient; (a) and (b) highlight the absorption and desorption parts of the plot, respectively.

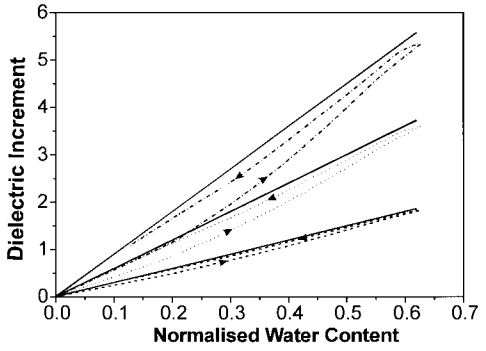

Figure 9 Computer simulated results for the dielectric increment dependence on the water content when the water content is varied by (right filled triangle) hydration and (left filled triangle) dehydration. The increment is calculated for three different coefficients of proportionality k. The solid lines represent the dielectric permittivity of a system with uniformly distributed water; (——), (· · · ·), (- · - · - ·) represent the results for a system with water content distributed through the sample's half length as shown in Figure 8, and three increasing values of k in respective order.

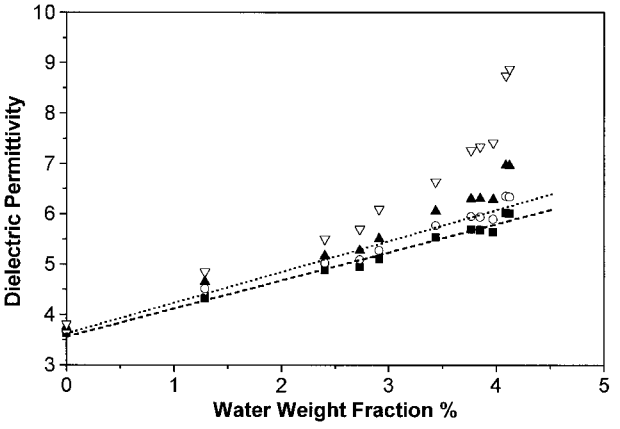

Figure 11 Dielectric permittivity measured at (■) 10 kHz, (○) 1 kHz, (▲)100 Hz, and (▽) 10 Hz as function of the water weight fraction. The data were obtained during exposure of sample F to 5% w/w NaCl solution at 65°C.

The change in the real dielectric permittivity with the water weight fraction is given in Figure 11. The traces replicate those for aging in deionized water for water weight fractions up to 4.2%. In the case of aging in salt solution, the water weight fractions do not exceed this value (Fig. 12).

The effect of salt in the aging solution on the water absorption behavior of the resin was discussed in Part I.[14] The two stages of absorption in the case of deionized water were attributed to (1) the process of moisture saturation of the epoxy matrix, and (2) diffusion of water into microcavities via an osmotic mechanism. The latter does not take place when the material is immersed in 5% w/w NaCl solution. The loss of weight from the samples exposed to salt solution was found to be due to removal of unreacted hardener rather than desorption of water; therefore, the water weight fraction was taken as constant on the second part of the plot.

A necessary condition for an osmotic mechanism to occur is the material to be impermeable to the solute. The comparison between the real dielectric permittivity of the samples aged in deionized water and salt solution measured as a func-

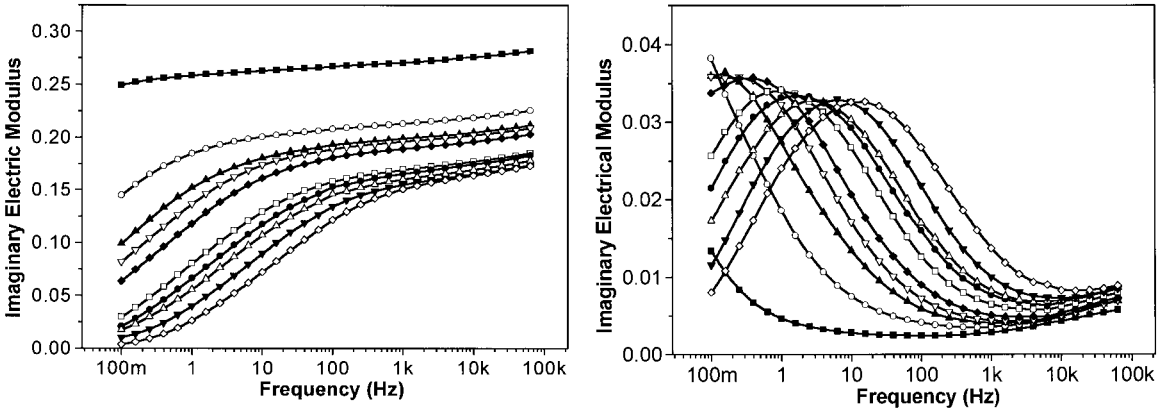

Figure 10 (a) Real and (b) imaginary electric modulii vs. frequency at different stages of aging of sample F in 5% w/w NaCl solution at 65°C. (■) represents the data measured before the start of the experiment; (○), (▲), (▽), (◆), (□), (●), (△), (▼), and (◇) after 21.75, 73.75, 94, 110, 280, 427, 593, 806, and 7700 h of aging, respectively.

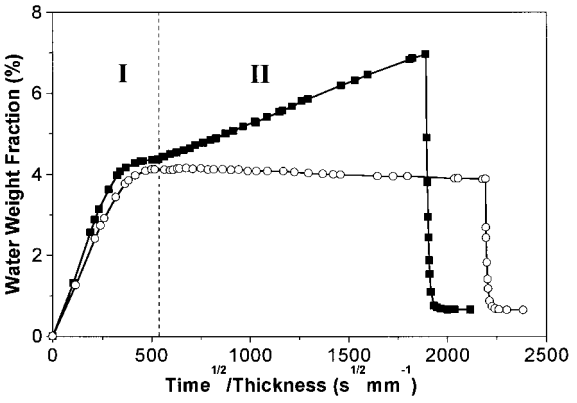

Figure 12 Water weight fraction as function of the ratio of the square root of time to the thickness of the sample for samples (■) C and (○) F.

tion of the water weight fraction is presented by Figure 13. It can be seen that there is no apparent influence of the presence of salt in the aging solution. The imaginary dielectric permittivity is also unaffected by the presence of salt, contrary to what would be expected if the material was permeable to the NaCl, leading to increased number of charge carriers in the system.

In Figure 2, the change of the frequency of the imaginary electric modulus peak with exposure time for the material aged in salt solution was compared to that for the material aged in deionized water. The time behavior of the glass transition temperature of both systems were identical. The samples exposed to deionized water absorbed almost twice the amount of water absorbed by the samples aged in salt solution for the given experimental time, but the difference is due to water that resides in cavities, and does not further affect the glass transition temperature.[15]

Figure 14 shows the change in the real dielectric permittivity of the material with the water

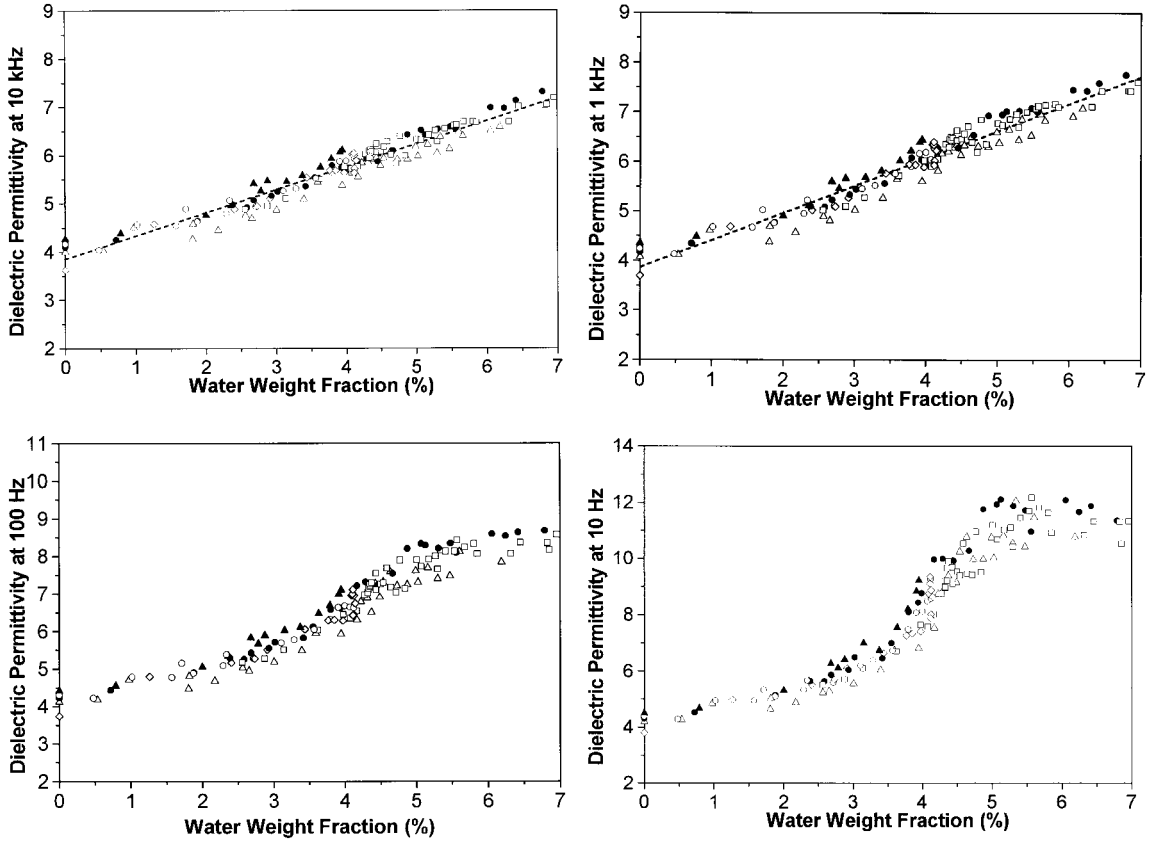

Figure 13 Real dielectric permittivity measured at (a) 10 kHz; (b) 1 kHz; (c) 100 Hz, and (d) 10 Hz as function of the water fraction. The water fraction was varied by immersing of the samples in deionized water/5% w/w NaCl solution. (△), (●), (□), (○), (▲), and (◇) represent the data obtained for sample A, B, C, D, E, and F, respectively. For samples A, B, D, and E the results collected during both absorption cycles are shown.

weight fraction after placing the material in an oven at 65°C following exposure to 5% w/w NaCl solution. Similarly to the former case of exposure to deionized water, the dielectric permittivity measured at frequencies above 1 kHz depends linearly on the water weight fraction with no apparent hysteresis of the hydration–dehydration cycle. The real permittivity measured at frequencies below 1 kHz strongly depends on the water profile within the sample, and thus on the departure point prior to dehydration, and therefore, is not presented.

During the first stage of the water absorption (up to 4.35% water weight fraction) the material can be seen as a medium with a real dielectric permittivity, $\epsilon^{(\mathrm{dry})}$, of the dry polymer, which contains molecularly dispersed water. During the second stage of absorption the material may be considered as a two-phase system: a filler (clustered water) with dielectric permittivity of 80 in a matrix (moisture saturated epoxy) with real dielectric permittivity $\epsilon|_{w=4.35\%}$. The two mixing stages are schematically presented in Figure 15.

Aldrich et al.[7] derived, from the stand point of the Clausius-Mossotti equation, the effect of molecularly dispersed water in an epoxy resin on the static dielectric permittivity to be

$$\varepsilon\left(w\right) - \varepsilon^{(\mathrm{dry})} = \frac{\varepsilon(w) + 2}{\varepsilon(\mathrm{dry}) + 2}\left(\frac{\varepsilon^{(\mathrm{dry})} + 2}{3}\right)^2 \left(\frac{\mu^2 N}{3kT}\right) f \tag{11}$$

where μ is the dipole moment of water, N is the number density of water molecules, k is Boltzmann's constant, T is the temperature, and f represents any fractional change of the observed water polarizability from its free, unassociated value. For small water fractions it was further shown

$$\varepsilon(w) - \varepsilon^{(\mathrm{dry})} = 4.0(\varepsilon^{(\mathrm{dry})} + 2)^2 f\rho w / T \tag{12}$$

where w is the water weight fraction and ρ is the density of the polymer.

The use of a nonstatic dielectric permittivity in analysis of the water absorption with the above equation could be justified if at the frequency and the temperature studied, the loss factor was sufficiently below its maximum value. One can see from Figure 1 that this condition is fulfilled for measurements performed at frequency of 10 kHz and ambient temperature.

For two-phase systems with host material characterized by dielectric permittivity of ϵ_1 and spherical inclusions with dielectric permittivity ϵ_2 and volume fraction v_2, Looyenga's[20] equation reads

$$\varepsilon = [\varepsilon_1^{1/3} + v_2\,(\varepsilon_2^{1/3} - \varepsilon_1^{1/3})]^3 \tag{13}$$

The dielectric permittivities in the above equation are the permittivities at high frequencies with respect to the MWS effect. The Sillar's equation for spherical dispersed phase[21] applied to the current system predicts a loss maxima of low intensity at approximately 1 kHz, so the use of the real dielectric permittivity measured at 10 kHz is justified again.

Figure 16 shows the real dielectric permittivity of the material measured at 10 kHz and compared with the theoretically predicted values using eq. (12) for $w = 4.35$ and eq. (13) for $w > 4.35$. The best fit to the data with eq. (12) was obtained for

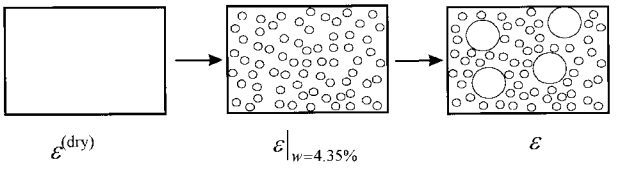

Figure 15 Schematic diagram representing the two mixing stages: molecularly dispersed water mixed into polymer matrix with permittivity $\epsilon^{(\mathrm{dry})}$ to form a background $\epsilon|_{w=4.35\%}$ and then clustered water with permittivity of 80 mixed into medium $\epsilon|_{w=4.35\%}$ to give apparent dielectric permittivity ϵ.

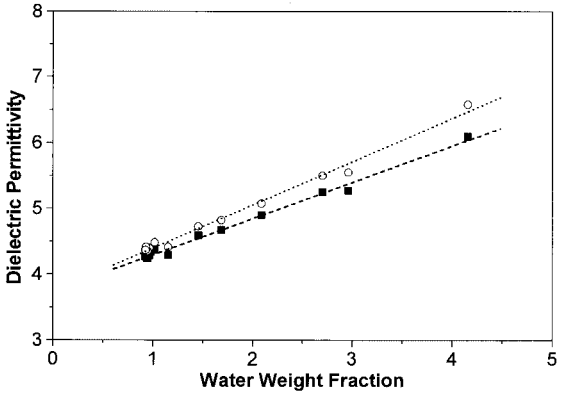

Figure 14 Dielectric permittivity measured at (■) 10 kHz and (○) 1 kHz as function of the water weight fraction. The data were obtained during the dehydration of sample F at 65°C.

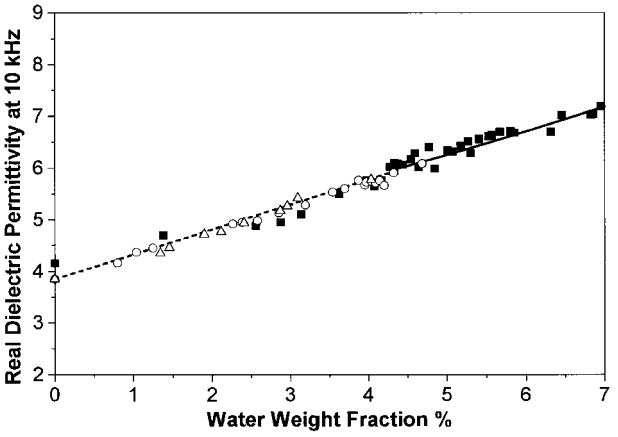

Figure 16 Dielectric permittivity at 10 kHz as function of the water weight fraction. The data for samples (■) C, (○) G, and (△) H aged in deionized water at 65, 60, and 50°C, respectively. The dashed and solid lines represent the theoretical values predicted by eq. (12) and eq. (13), respectively.

$f = 0.67$—a value that is within the range of those reported for various epoxy systems.[7]

Fortuitously, with both models similar slopes are obtained for the composition dependence of dielectric permittivity.

The apparent linearity of the composition dependence allows the diffusion coefficient of the water to be calculated from the data for the dielectric increment. For semi-infinite media the solution of the second Fick's law is

$$\frac{M_t}{M_\infty} = 1 - \frac{8}{\pi^2}\sum_{n=0}^{\infty}\frac{1}{(2n+1)^2}\exp\left[-\frac{Dt}{l^2}\pi^2(2n+1)^2\right] \quad (14)$$

where M_t denotes the total amount of diffusing substance, which has entered a sheet with thickness l at time t, M_∞ is the corresponding quantity at equilibrium, and D is the diffusion coefficient. From the proportionality of the real dielectric permittivity to the water content it follows that

$$\frac{\Delta\varepsilon_t'}{\Delta\varepsilon_\infty'} = 1 - \frac{8}{\pi^2}\sum_{n=0}^{\infty}\frac{1}{(2n+1)^2}\exp\left[-\frac{Dt}{l^2}\pi^2(2n+1)^2\right] \quad (15)$$

where $\Delta\epsilon'_t$ is the dielectric increment at time t, and $\Delta\epsilon'_\infty$ is the dielectric increment at equilibrium water content.

Figure 17 presents the comparison between the data for the normalized water content and the normalized real dielectric permittivity measured at 10 kHz. The normalized water content is defined as

$$\text{Normalized Water Content} = \frac{W_t}{W_\infty^*} \quad (16)$$

where W_t is the amount of water that has entered the sample at time t and W_∞* is taken as (1) the maximum amount of water lost from a sample in the case of a desoprtion experiment; or (2) the amount of water that is absorbed by a sample at the end of the first stage of absorption in the case of immersion in deionized water; and (3) maximum amount of water absorbed by a sample in the case of immersion in 5% w/w NaCl solution. The normalized real dielectric permittivity is defined as

$$\text{Normalized Real Dielectric Permittivity} = \frac{\Delta\varepsilon_t'}{\Delta\varepsilon_\infty'^*} \quad (17)$$

where $\Delta\epsilon'_t$ is the dielectric increment at time t and $\Delta\epsilon'_\infty$* is (1) the maximum dielectric increment in case of desorption or immersion in 5% w/w NaCl solution; or (2) dielectric increment at the end of the first stage of absorption in the case of immersion in deionized water. It can be seen that the traces for the normalized dielectric permittivity closely follow those for the normalized water content. In the case of exposure of the material to 5%w/w NaCl solution the normalized water content reaches a maximum and then slowly decreases, but the normalized dielectric permittivity remains invariant. The decrease in the value of the normalized water content, as was noted earlier, is due to desorption of unreacted hardener, but not loss of water from the sample. The dicyandiamide has a low dielectric permittivity; therefore, the measured permittivity is unaffected by its leaching from the material.

The solid line in Figure 17 represents the best fit to the dielectric data obtained with eq. (15). In the case of exposure to deionized water, eq. (15) was applied only to the data obtained during the first stage of the water absorption. The values of the diffusion coefficients used to obtain best fit to the dielectric data are given in Table II, compared to the values of the diffusion coeficients obtained from the best fit with eq. (14) to the data for the

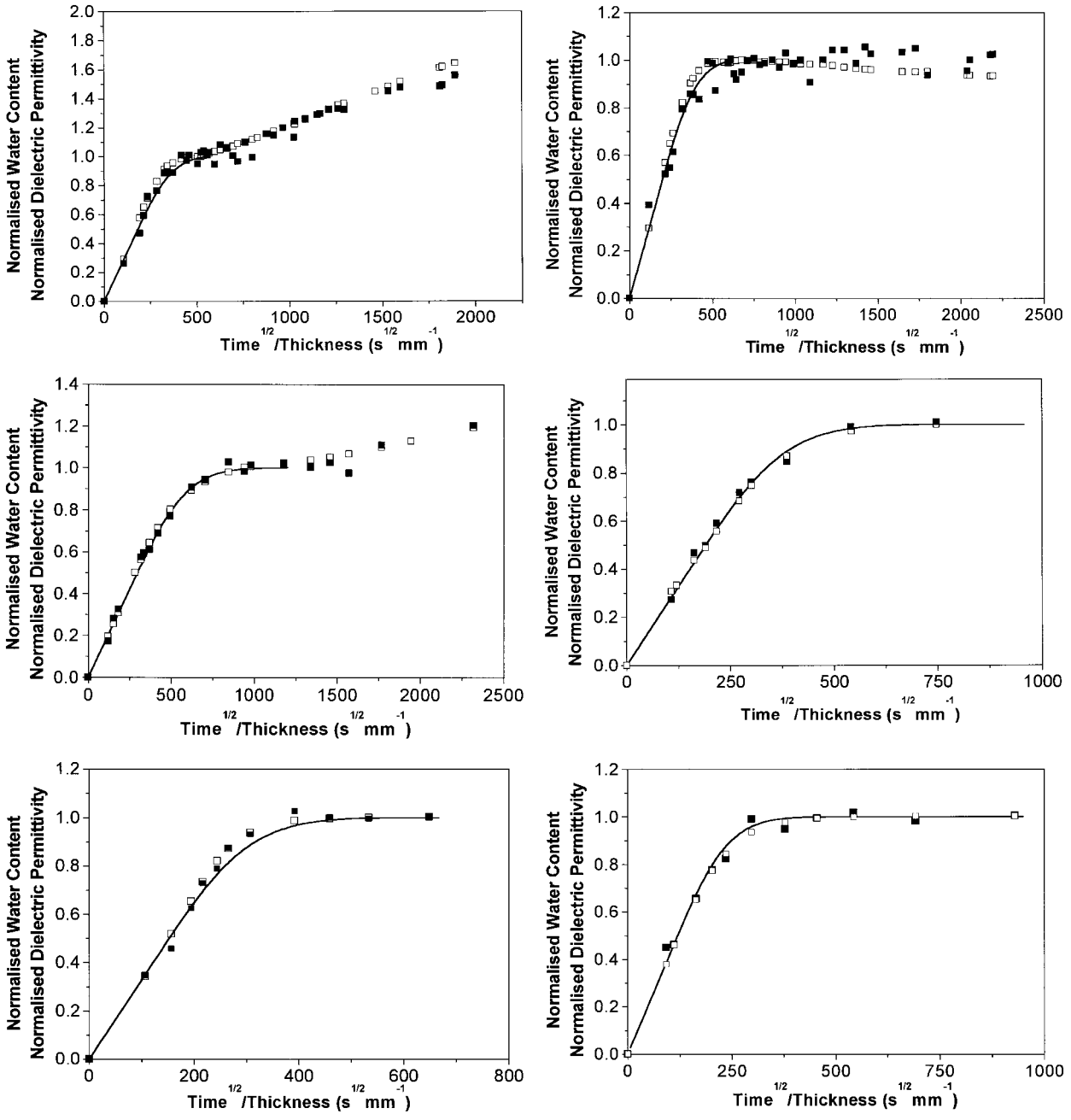

Figure 17 Normalized dielectric permittivity measured at 10 kHz (■) and normalized water content (□) vs. the ratio of the square root of time to the thickness of the sample measured during (a, b, c, d) hydration of samples C, F, G, and H, respectively; (e, f) dehydration of samples C and F, respectively. The solid line represents the best fit obtained with eq. (15) to the data for the normalized dielectric permittivity obtained during the first 600 h of exposure to deionized water/5% w/w NaCl solution—the time necessary for the moisture saturation.

water content. There is a good agreement between both sets of data. One can see that the error in the diffusion coefficient obtained from dielectric data is smaller when the dielectric permittivity is measured during desorption than when it is measured during absorption.

Figure 18 represents the normalized water content measured at 65°C compared to that mea-

Table II Diffusion Coefficients Obtained for the Water Absorption/Desorption from Both Gravimetric and Dielectric Data

	Absorption D× 10^{-8} (cm^2 s^{-1})		Desorption D× 10^{-8} (cm^2 s^{-1})	
Sample	Weight	Real Permittivity @10 kHz	Weight	Real Permittivity @10 kHz
$A^{(II)}$	2.7	1.4	2.6	2.5
$B^{(II)}$	3.1	2.0	2.2	1.9
C	1.8	1.5	2.3	2.1
$D^{(II)}$	2.0	1.5	3.2	3.5
$E^{(II)}$	2.8	1.9	3.2	3.6
F	1.5	1.3	3.2	3.4
G	1.3	1.3	—	—
H	0.60	0.56	—	—

The symbol (II) indicates the data obtained from the second sorption cycles.

sured at 50 and 60°C. The increase in the exposure temperature does not significantly affect the amount of water nessecary for saturation of the epoxy matrix, but results in an increase in the rate of both stages of the absorption process.

The activation energy of diffusion for the first stage of the absorption is calculated from the slope of the plot of log(D) vs. the reciprocal value of the temperature (Fig. 19). The values calculated from the gravimetric and dielectric data are 28 and 26 kJ/mol, respectively.

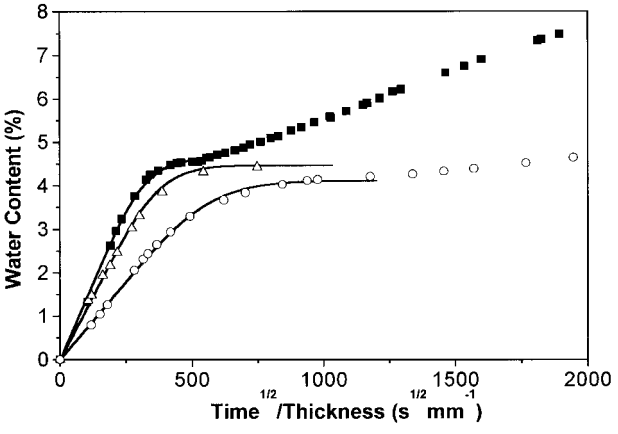

Figure 18 Water content as a function of the ratio of the square root of time to the thickness of the sample for samples (■) C, (△) G, and (▼) H exposed to deionized water at 65, 60, and 50°C, respectively. The solid lines represent the best fit obtained with Fickian model to the data obtained during the first stage of absorption.

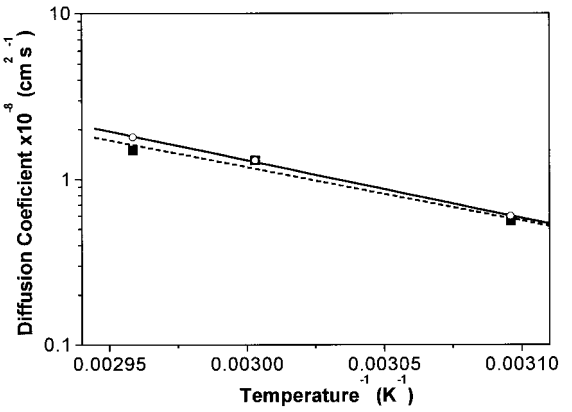

Figure 19 Diffusion coefficient calculated from (○) gravimetric and (■) dielectric data as a function of the reciprocal value of the temperature. The solid and the dashed lines represent linear fit to both sets of data, respectively.

CONCLUSIONS

The effects of water absorption on the dielectric response of DGEBA/DICY epoxy resin were studied. No effect of the hygrothermal history, presence of salt, or aging temperature on the dielectric permittivity was apparent.

Water absorbed at levels up to 4.3% weight fraction is molecularly dispersed throughout the resin, and its dielectric contribution is close to that predicted by Onsager for unassociated water molecules. The water absorbed at levels greater than 4.3% weight fraction remains in microcavities, formed as a result of the aging. The dielectric contribution of this clustered water is well described by Looyenga's mixture rule for spherical inclusions.

The resin is impermeable to the NaCl, and its presence in the aging solution at 5% w/w prevents the microcavity growth and thus does not allow water absorption at levels higher than 4.1% weight fraction.

The real dielectric permittivity measured at 10 kHz could be used to monitor the level of water absorption by the epoxy resin, and allows the activation energy of diffusion to be calculated independently.

Ivanova thanks Alcan International Ltd. (Banbury) for a studentship. The authors thank Dr. D. Hayward for helpful discussion.

REFERENCES

1. Hastead, J. B. Aqueous Dielectrics; Chapman and Hall: London, 1973.
2. Topp, G. C.; Davis, J. L.; Annan, A. O. Water Resour Res 1980, 16, 574.
3. Maffezzoli, M.; Peterson, L.; Seferis, J. C.; Kenney, J.; Nicolais, L. Polym Eng Sci 1995, 33, 75.
4. van Beek, L. K. H. Prog Dielectrics 1967, 7, 69.
5. Maxwell, D.; Pethrick, R. A. J Appl Polym Sci 1983, 28, 2363.
6. Woo, M.; Piggott, M. R. J Composites Technol Res 1987, 9, 101.
7. Aldrich, P. D.; Thurow, S. K.; McKennon, M. J. Polymer 1987, 28, 2289.
8. Bosma, T. J.; Lebey, T.; Pouilles, V.; Chenerie, I.; Ai, B.; Rieux, N. J Phys D Appl Phys 1995, 28, 1180.
9. Lu, X.; Xu, G.; Hofstra, P. G.; Bajcar, R. C. J Polym Sci Part B Polym Phys 1998, 36, 2259.
10. Etienne, S.; Stochmil, C.; Bessede, J. L. J Alloy Compd 2000, 310, 368.
11. Korzhenko, A.; Tabellout, M.; Emery, J. R. Mater Chem Phys 2000, 65, 253.
12. Pethrick, R. A.; Hollins, E. Q.; McEwan, I.; Pollok, E. A.; Hayward, D. Polym Int 1996, 39, 275.
13. Hayward, D.; Hollins, E.; Johncock, P.; McEWwan, I.; Pethrick, R. A.; Pollock, E. A. Polymer 1997, 38, 1151.
14. Ivanova, K. I.; Pethrick, R. A.; Affrossman, S. J Appl Polym Sci, accepted.
15. Ivanova, K. I.; Pethrick, R. A.; Affrossman, S. J Appl Polym Sci, accepted.
16. Hayward, D.; Gawayne, M.; Mahboubian-Jones, B.; Pethrick, R. A. J Phys E Sci Instrum 1984, 17, 683.
17. Ammbrus, J. H.; Moynihan, C. T.; Macedo, P. B. J Phys Chem 1972, 76, 3287.
18. Ishida, Y. Kolloidn Zh 1960, 171, 149.
19. Macedo, P. B.; Moynihan, C. T.; Bose, R. Phys Chem Glasses 1972, 13, 171.
20. Looyenga, H. Physica 1965, 31, 401.
21. Boyle, M. H. Colloid Polym Sci 1985, 263, 51.